

Franck-Condon factors based on anharmonic vibrational wave functions of polyatomic molecules

Valerie Rodriguez-Garcia

Quantum Theory Project, Department of Chemistry, University of Florida, Gainesville, Florida 32611-8435

Kiyoshi Yagi and Kimihiko Hirao

Department of Applied Chemistry, School of Engineering, The University of Tokyo, Tokyo 113-8656, Japan and CREST, Japan Science and Technology Agency, Saitama 332-0012, Japan

Suehiro Iwata

Center for Quantum Life Sciences, Hiroshima University, Hiroshima 739-8526, Japan and Graduate School of Science, Hiroshima University, Hiroshima 739-8526, Japan

So Hirata^{a)}

Quantum Theory Project, Department of Chemistry, University of Florida

(Received 10 April 2006; accepted 9 May 2006; published online 7 July 2006)

Franck-Condon (FC) integrals of polyatomic molecules are computed on the basis of vibrational self-consistent-field (VSCF) or configuration-interaction (VCI) calculations capable of including vibrational anharmonicity to any desired extent (within certain molecular size limits). The anharmonic vibrational wave functions of the initial and final states are expanded unambiguously by harmonic oscillator basis functions of normal coordinates of the respective electronic states. The anharmonic FC integrals are then obtained as linear combinations of harmonic counterparts, which can, in turn, be evaluated by established techniques taking account of the Duschinsky rotations, geometry displacements, and frequency changes. Alternatively, anharmonic wave functions of both states are expanded by basis functions of just one electronic state, permitting the FC integral to be evaluated directly by the Gauss-Hermite quadrature used in the VSCF and VCI steps [Bowman *et al.*, *Mol. Phys.* **104**, 33 (2006)]. These methods in conjunction with the VCI and coupled-cluster with singles, doubles, and perturbative triples [CCSD(T)] method have predicted the peak positions and intensities of the vibrational manifold in the \tilde{X}^2B_1 photoelectron band of H₂O with quantitative accuracy. It has revealed that two weakly visible peaks are the result of intensity borrowing from nearby states through anharmonic couplings, an effect explained qualitatively by VSCF and quantitatively by VCI, but not by the harmonic approximation. The \tilde{X}^2B_2 photoelectron band of H₂CO is less accurately reproduced by this method, likely because of the inability of CCSD(T)/cc-pVTZ to describe the potential energy surface of open-shell H₂CO⁺ with the same high accuracy as in H₂O⁺. © 2006 American Institute of Physics. [DOI: 10.1063/1.2209676]

I. INTRODUCTION

The evaluation of *anharmonic* Franck-Condon (FC) integrals,^{1,2} useful in spectral simulations of various kinds, involves three computational steps: one that performs electronic structure calculations and furnishes the potential energy functions (PEFs), one that computes anharmonic vibrational wave functions using these PEFs, and one that combines these with harmonic FC integrals and generates simulated anharmonic spectra. All three components deal with nearly intractable many-body problems. Nonetheless, it is generally agreed that electronic structure theory now offers hierarchies of systematic and converging sequence of approximations, such as configuration-interaction (CI), many-body perturbation (MBPT), and coupled-cluster (CC) methods, by which increasingly accurate PEFs can be obtained.

Parallel with these advances, converging series of many-

body methods for molecular vibrations have been developed by a smaller group of investigators. The self-consistent-field (SCF) method for molecular vibrations (VSCF), championed by Bowman³ and by Ratner and Gerber,⁴ followed by the VCI,⁵ VMBPT,⁶ and VCC (Ref. 7) methods (with the letter “V” standing for “vibrational”), accounts for intramode anharmonic effects and mode-mode anharmonic couplings to any desired extent. They rely on unbiased and well-defined expansion bases (i.e., harmonic oscillator wave functions along normal coordinates), thereby obviating *ad hoc* coordinate systems that may need to be tailored to individual problems.

In compliance with the *model chemistry* concept of Pople *et al.* (see, e.g., Ref. 8), these electronic and vibrational structure methods, once integrated, constitute an unambiguous, generally applicable computational procedure yielding anharmonic vibrational frequencies (including such effects as tunneling and Fermi resonances), vibrationally averaged structure and molecular properties, etc., that are di-

^{a)}Author to whom correspondence should be addressed. Electronic mail: hirata@qtp.ufl.edu

rectly comparable with experimental measurements. Furthermore, the systematic nature of the many-mode and basis set expansions enables the convergence of calculated quantities to be achieved in principle. The general applicability to polyatomic molecules is ensured by recent advances that address the high dimensionality of PEFs. The prime examples are the many-mode expansions of PEFs (the so-called n MR method) proposed by Carter *et al.*,⁹ the *direct* vibrational SCF that uses pointwise numerical values of PEFs and avoids their analytic representations by Chaban *et al.*,¹⁰ and the modified Shepard interpolation of PEFs by quartic force fields (QFFs) at a few reference geometries advocated by Yagi *et al.*¹¹

This article presents a machinery for evaluating anharmonic FC integrals and validates it through the simulations of vibrationally resolved photoelectron spectra of H₂O and H₂CO. It inherits the aforementioned strengths of modern electronic and vibrational many-body methods; the levels of approximations used in describing electronic and vibrational wave functions can be independently raised. There are a number of previous reports on efficient computational methods for harmonic FC integrals for polyatomic molecules.^{12–26} In addition to the information obtainable from these, our method can account for the anharmonic frequencies of fundamentals, overtones, and combination tones (and possibly the presence of dissociation limits) and intensity redistributions due to anharmonic couplings between normal modes. As such, it will be crucial for the quantitative interpretation of vibrational progressions in optical absorption, fluorescence, photoelectron spectra, and resonance Raman intensities and their excitation profiles (see, e.g., Ref. 27 for a harmonic FC analysis of Raman intensities). The limitation of our method is that it currently cannot describe the spectral features ascribable to nonadiabatic (vibronic) coupling effects, the Renner-Teller and Jahn-Teller effects, or rovibrational coupling.

II. OTHER RELATED THEORETICAL STUDIES

Mok and co-workers^{28–31} scanned the PEFs of triatomic molecules with accurate electronic structure methods and expressed them by polynomial functions of bond lengths and bond angles. They solved the vibrational Schrödinger equations defined by the complete Watson Hamiltonian and these PEFs by a VCI method employing harmonic oscillator wave functions as basis functions. This method has been applied to HSiF,²⁹ HPCI,³⁰ TeO₂,³¹ etc., demonstrating impressive agreement between theory and experiment. Our method uses a similar strategy for the last step (the VCI method based on harmonic oscillator wave functions to compute FC integrals), while avoiding molecule-specific coordinate systems for a PEF polynomial fit, by virtue of the VSCF and VCI methods in conjunction with the direct method or QFF approximation.

Bowman *et al.* reported a computational scheme to evaluate FC integrals by using anharmonic VSCF and VCI wave functions as implemented in their MULTIMODE program and applied it to the photoelectron spectra of CF₃.³² They expressed both initial- and final-state PEFs in terms of the equilibrium geometry and normal coordinates of the initial state, permitting the complete and facile inclusions of

geometry displacements, frequency changes, and normal mode transformations between the two states in FC integrals, without having to form a Duschinsky rotation matrix. We explore the same approach and also another, complementary one in which initial- and final-state PEFs are expanded by their respective normal mode harmonic oscillators. We will validate both approaches by comparing the results.

Hazra *et al.*^{33–36} proposed expanding the final-state PEF only in the immediate vicinity of the equilibrium geometry of the initial state, i.e., in the only region where they were expected to be relevant, according to the short-time picture of spectroscopy. This is related to the aforementioned approach of Bowman *et al.*, which will also be considered in this work. Luis *et al.*^{37,38} considered the effect of anharmonicity on FC integrals by including the effects of cubic force constants through first- or second-order perturbation theory. One merit of our method (and that of Bowman *et al.*), as compared to the methods of Hazra *et al.* or Luis *et al.*, may be that it includes strong mode-mode anharmonic couplings, which can be beyond the validity of the perturbation theory. The streamlined PEF samplings of Hazra *et al.* and Luis *et al.*, on the other hand, may render their methods more easily applicable to greater vibrational degrees of freedom. Furthermore, Hazra *et al.* considered the nonadiabatic (vibronic) effects on their calculated spectra.

III. DETAILS OF THE CALCULATION

A. Potential energy functions

Throughout the present study, we have employed the closed- and open-shell (spin-unrestricted) CCSD(T) (coupled-cluster with singles, doubles, and perturbative triples) theory^{39,40} in conjunction with the cc-pVTZ (Cartesian) basis set⁴¹ (all electrons correlated) as implemented in the ACES II computer code.⁴² With this, only the neutral and cationic species in their ground states can be reliably studied. The PEFs of these species have been generated by one or both of the following two ways by using the SINDO computer code⁴³ written by Yagi.

We have invoked the direct algorithm advocated by Chaban *et al.*¹⁰ and by Yagi *et al.*⁴⁴ and tabulated the numerical values of the PEF, point by point, on a multidimensional, rectangular grid based on the normal coordinates. The grid has 11 points (including zero displacement) along each normal mode that have been distributed according to the Gauss-Hermite quadrature rule (which may be viewed as one form of the discrete-variable representation of Light and Carrington).⁴⁵ The program performing this step has taken advantage of the C_{2v} symmetry of the molecules to avoid unnecessary electronic structure calculations at symmetrically nonunique geometries. It has also automatically interpolated or extrapolated energies at several geometries where energy calculations have failed. Such precautionary measures are crucial when thousands of electronic structure calculations are performed, and a few of them are almost certain to fail at the most highly strained geometries.

A considerably less expensive alternative exists, which is to expand the PEFs in Taylor series at equilibrium geometries and to use the series truncated after the fourth-order

derivative term for subsequent anharmonic vibrational analyses. This has been shown to be remarkably useful when one is interested in low-lying and relatively harmonic vibrational modes. We have relied on this approach (QFF), which has been introduced by Yagi *et al.*⁴⁶ in the context of the VSCF and VCI, for the molecules studied here. This should be distinguished from the fourth-order perturbation anharmonic corrections to harmonic frequencies and wave functions; unlike those, our VSCF and VCI schemes can handle strong anharmonic couplings among normal modes. The quartic and lower-order force constants have been computed by carrying out a number of energy calculations at geometries with displacements along normal modes⁴⁶ (see also Ref. 47). Step sizes that govern the accuracy and stability of numerical differentiation have been optimized automatically according to the harmonic frequencies.⁴⁶ Again, the program has been written that automates the entire procedure while maximizing the use of point group symmetry.

In either of the aforementioned approaches, we have occasionally imposed the truncation of many-body expansion of anharmonic couplings between normal modes. In this n -mode coupling approximation (n MR) of Carter *et al.*,⁹ energy calculations at geometries with simultaneous displacements along more than n normal modes become unnecessary. Consequently, the number of energy calculations reduces from N^m to mere ${}_m C_n \times N^m$, where N is the number of displacements along each normal mode and m is the vibrational degrees of freedom. It may be said that the n MR approximation is what makes the VSCF and VCI calculations for larger polyatomic molecules manageable. The n MR approximation has been integrated into the SINDO program⁴³ that has generated the PEFs either by the direct or QFF approach. We have invoked 2MR approximation with the direct algorithm and 3MR approximation with the QFF approximation for H₂CO and H₂CO⁺.

B. Anharmonic vibrational analysis

The VSCF wave function for quantum state $|\nu_1, \dots, \nu_n\rangle$ (with n being the vibrational degrees of freedom) is a product of functions of normal coordinates Q_1, \dots, Q_n , i.e.,

$$\Psi_{\nu_1 \dots \nu_n}^{\text{VSCF}}(Q_1, \dots, Q_n) = \prod_{i=1}^n \varphi_{\nu_i}(Q_i). \quad (1)$$

Each one-mode function or *modal* (in Bowman's notation) is, in turn, a linear combination of the harmonic oscillator (HO) wave functions along normal coordinates

$$\varphi_{\nu_i}(Q_i) = \sum_{w_i=1}^N C_{\nu_i}^{w_i} \chi_{w_i}^{\text{HO}}(Q_i), \quad (2)$$

where the expansion coefficients $\{C_{\nu_i}^{w_i}\}$ are determined so that the expectation value $\langle \Psi_{\nu_1 \dots \nu_n}^{\text{VSCF}} | \hat{H} | \Psi_{\nu_1 \dots \nu_n}^{\text{VSCF}} \rangle$ of the Hamiltonian \hat{H} becomes stationary. Parameter N ultimately controls the accuracy of the VSCF wave functions and energies ($N=11$ has been used). It corresponds to the highest rank of Hermitian polynomials in the normal mode harmonic oscillator wave functions $\{\chi_{w_i}^{\text{HO}}\}$ and also to the number of grid points in the Gauss-Hermite quadrature (*vide ante*).

The VCI calculations are performed based either on VSCF or harmonic oscillator wave functions

$$\Psi_I^{\text{VCI}}(Q_1, \dots, Q_n) = \sum_{J=1}^M C_I^J \Psi_J^{\text{VSCF}}(Q_1, \dots, Q_n), \quad (3)$$

$$\Psi_I^{\text{VCI}}(Q_1, \dots, Q_n) = \sum_{J=1}^M C_I^J \Psi_J^{\text{HO}}(Q_1, \dots, Q_n), \quad (4)$$

where I and J are indices representing quantum state $|\nu_1, \dots, \nu_n\rangle$ and

$$\Psi_{\nu_1 \dots \nu_n}^{\text{HO}}(Q_1, \dots, Q_n) = \prod_{i=1}^n \chi_{\nu_i}^{\text{HO}}(Q_i). \quad (5)$$

Again, the expansion coefficients $\{C_I^J\}$ are determined variationally. The expansion of Eq. (3) is more rapidly convergent than that of Eq. (4) with respect to M (the number of the many-mode basis functions). The VCI method selects configurations not according to excitation ranks, but to an energy-based criterion. In our study, we have included the first 1000 and 3000 lowest-energy configurations for H₂O (H₂O⁺) and H₂CO (H₂CO⁺), respectively. For H₂O (H₂O⁺), this virtually amounts to the full VCI (because the number of all possible configurations is $11^3=1331$). All the VSCF and VCI calculations have been performed with the SINDO program.⁴³

C. Franck-Condon factors

The intensities of optical absorption and fluorescence spectral bands, photoelectron bands, resonance Raman scattering bands, etc., are governed mostly by the FC integrals, i.e., the overlap integrals between vibrational wave functions of two different electronic states. We have calculated them using the following two schemes.

In scheme A, both the VSCF and VCI anharmonic vibrational wave functions are expanded by the harmonic oscillator wave functions along normal modes [Eqs. (1) and (2) or Eqs. (4) and (5)]. Hence the FC integrals of the VSCF wave functions are related to those between the harmonic wave functions by

$$\begin{aligned} & \langle \Psi_{\nu_1 \dots \nu_n}^{\text{VSCF}}(Q_1, \dots, Q_n) | \Psi_{\nu'_1 \dots \nu'_n}^{\text{VSCF}}(Q'_1, \dots, Q'_n) \rangle \\ &= \left\langle \prod_{i=1}^n \varphi_{\nu_i}(Q_i) \left| \prod_{j=1}^n \varphi_{\nu'_j}(Q'_j) \right. \right\rangle \\ &= \left\langle \prod_{i=1}^n \sum_{w_i=1}^N C_{\nu_i}^{w_i} \chi_{w_i}^{\text{HO}}(Q_i) \left| \prod_{j=1}^n \sum_{w'_j=1}^N C_{\nu'_j}^{w'_j} \chi_{w'_j}^{\text{HO}}(Q'_j) \right. \right\rangle \\ &= \sum_I \sum_J \left(\prod_{i=1}^n C_{\nu_i}^{w_i} \right) \left(\prod_{j=1}^n C_{\nu'_j}^{w'_j} \right) \\ & \quad \times \langle \Psi_I^{\text{HO}}(Q_1, \dots, Q_n) | \Psi_J^{\text{HO}}(Q'_1, \dots, Q'_n) \rangle, \quad (6) \end{aligned}$$

where the primes underscore the differences in normal modes, anharmonic wave functions, etc., between the initial and final states; I represents quantum state $|w_1, \dots, w_n\rangle$; and J stands for $|w'_1, \dots, w'_n\rangle$. Similarly, the FC integrals of the

VCI wave functions are also written as linear combinations of harmonic FC integrals as follows:

$$\begin{aligned} & \langle \Psi_I^{\text{VCI}}(Q_1, \dots, Q_n) | \Psi_K^{\text{VCI}}(Q'_1, \dots, Q'_n) \rangle \\ &= \left\langle \sum_{J=1}^M C_I^J \Psi_J^{\text{HO}}(Q_1, \dots, Q_n) \middle| \sum_{L=1}^M C_K'^L \Psi_L^{\text{HO}}(Q'_1, \dots, Q'_n) \right\rangle \\ &= \sum_{J=1}^M \sum_{L=1}^M C_I^J C_K'^L \langle \Psi_J^{\text{HO}}(Q_1, \dots, Q_n) | \Psi_L^{\text{HO}}(Q'_1, \dots, Q'_n) \rangle. \end{aligned} \quad (7)$$

The multidimensional FC integrals for the harmonic vibrational wave functions $\langle \Psi_I^{\text{HO}} | \Psi_J^{\text{HO}} \rangle$ have been obtained by using the algorithm of Kupka and Cribb¹⁸ that uses recursion relations. The underlying ideas of the procedure have been proposed originally by Sharp and Rosenstock.¹² We have used the computer code written by Yamaguchi *et al.*,⁴⁸ later made applicable to greater vibrational degrees of freedom by Kishi and Iwata, and distributed by Iwata.⁴⁹ This scheme needs to take into account the proper transformation of normal modes (the Duschinsky rotation⁵⁰), displacements of the equilibrium geometries, and frequency changes between the initial and final states. Although the VCI with VSCF wave functions as a basis is more rapidly convergent than that with harmonic oscillator wave functions, we have invoked the latter in scheme A [Eq.(7)] because the advantages brought about by the VSCF will be cancelled by the use of harmonic FC integrals.

In scheme B, we have employed the harmonic oscillator wave functions of one electronic state to expand the VSCF wave functions (or their modals) of *both the initial and final* electronic states (in this work, the harmonic oscillator wave functions of the initial state are chosen as a basis). This idea has been explored independently by Bowman *et al.* very recently.³² The VCI wave functions of both states have, in turn, been expanded by these VSCF wave functions according to Eq. (3). Unlike the usual modal expansions that use the harmonic oscillator wave functions of respective electronic states, this is expected to work only when the changes in the equilibrium geometries and (harmonic) frequencies between the two states are modest.

Then the FC integrals of the VSCF and VCI wave functions are greatly simplified to

$$\langle \Psi_{v_1 \dots v_n}^{\text{VSCF}}(Q_1, \dots, Q_n) | \Psi_{v'_1 \dots v'_n}^{\text{VSCF}}(Q_1, \dots, Q_n) \rangle = \prod_{i=1}^n \sum_{w_i=1}^N C_{v_i}^{w_i} C_{v'_i}^{w_i}, \quad (8)$$

$$\begin{aligned} & \langle \Psi_I^{\text{VCI}}(Q_1, \dots, Q_n) | \Psi_K^{\text{VCI}}(Q_1, \dots, Q_n) \rangle \\ &= \sum_J^M \sum_L^M C_I^J C_K'^L \langle \Psi_J^{\text{VSCF}}(Q_1, \dots, Q_n) | \Psi_L^{\text{VSCF}}(Q_1, \dots, Q_n) \rangle, \end{aligned} \quad (9)$$

by virtue of the orthonormality of the harmonic oscillator wave functions that are associated with the *single*, initial-state PEF. The advantage of this scheme is that the multidimensional FC integrals are now reduced to the products of

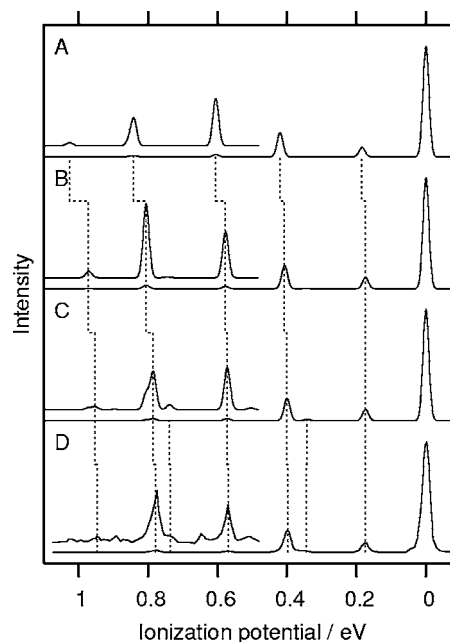


FIG. 1. Vibrational progression of the \tilde{X}^2B_1 photoelectron band of H_2O (zero of energy is taken as the 0-0 transition position). Calculations based on (A) the harmonic approximation, (B) VSCF (direct) wave functions, and (C) VCI (direct) wave functions are shown in comparison to (D) experiment (Ref. 51). The insert has been multiplied by 20. Each of the theoretical photoelectron peaks has been convoluted with a Gaussian function of FWHM of 0.02 eV.

one-dimensional integrals, which can be rapidly evaluated by quadratures. It does not require the explicit transformation of normal modes and hence the computer implementation is much more facile than those involving harmonic oscillator FC integrals with normal mode rotations.

The question is whether the harmonic oscillator basis (or, equivalently, Gauss-Hermite quadrature) for the initial-state PEFs can achieve adequate accuracy in integrating vibrational wave functions of the final-state PEFs. As we shall see in the next section, as few as 11 harmonic oscillators for the basis set can achieve reasonably high accuracy in FC integral evaluations for the examples studied here (which involve only modest normal mode rotations and geometry and frequency changes).

IV. RESULTS AND DISCUSSION

Several assumptions have been made in the following comparison between theory and experiment. First, the intensities of a single vibrational system of photoelectron spectra are assumed proportional to the square of FC integrals. In other words, the electronic part of the transition dipole moments is assumed constant for the energy range considered (the Herzberg-Teller expansion of the transition dipole moments has not been invoked). Second, the nonadiabatic (vibronic) effects are assumed negligible.

A. \tilde{X}^2B_1 state of H_2O^+

The experimental spectrum shown in Fig. 1 is the lowest-energy photoelectron band assignable to the \tilde{X}^2B_1 state of H_2O^+ . This is a part of a wider spectrum reported by

TABLE I. Relative positions (ν in cm^{-1}), relative intensities (I), and assignment of vibrational progression of the \tilde{X}^2B_1 photoelectron band of H_2O obtained from the CCSD(T)/cc-pVTZ method.

Assignment ^a	Harmonic		VSCF (QFF) ^b		VSCF (direct) ^b		VCI (QFF) ^b		VCI (direct) ^b		VCI (direct) ^c		Expt. ^d	
	ν	I	ν	I	ν	I	ν	I	ν	I	ν	I	ν	I
0 0 0 (0_0)	0	1.000	0	1.000	0	1.000	0	1.000	0	1.000	0	1.000	0	1.000
0 1 0 (2_1)	1487	0.086	1402	0.106	1411	0.103	1397	0.104	1407	0.101	1406	0.107	1407,1408.42 ^e	0.089
0 2 0 (2_2)	2974	0.000	2763	0.002	2789	0.002	2738	0.007	2766	0.011	2763	0.012	2775,2771.27 ^e	0.010
1 0 0 (1_1)	3392	0.217	3299	0.212	3288	0.210	3254	0.209	3230	0.202	3231	0.200	3205,3213.00 ^f	0.193
0 0 1 (3_1)	3450	0.000	3320	0.000	3297	0.000	3297	0.000	3264	0.000	3261	0.000	3253.03 ^f	
0 3 0 (2_3)	4461	0.000	4071	0.000	4137	0.000	3989	0.001	4069	0.001	4071	0.001	4085	0.003
1 1 0 ($1_1 2_1$)	4879	0.021	4645	0.023	4661	0.021	4598	0.022	4616	0.019	4616	0.020	4593	0.016
1 2 0 ($1_1 2_2$)	6366	0.000	5949	0.000	6003	0.000	5893	0.001	5955	0.002	5955	0.003	5936	0.003
2 0 0 (1_2)	6785	0.012	6563	0.025	6501	0.027	6486	0.024	6333	0.017	6342	0.022	6280	0.023
0 0 2 (3_2)	6899	0.002	6589	0.006	6480	0.007	6581	0.001	6498	0.007	6502	0.007		
2 1 0 ($1_2 2_1$)	8272	0.002	7839	0.003	7837	0.003	7741	0.002	7679 ^g	0.001	7681 ^g	0.002	7639	0.003

^aQuantum numbers of ν_1 (OH symmetric stretch; A_1), ν_2 (OH_2 scissors; A_1), and ν_3 (OH antisymmetric stretch; B_2).

^bScheme A based on the Franck-Condon integrals of harmonic oscillator wave functions (see text).

^cScheme B based on the anharmonic wave functions of H_2O and H_2O^+ both expanded by the harmonic oscillator wave functions of H_2O (see text).

^dReference 51, unless otherwise stated.

^eReference 55.

^fReference 54.

^gPrimarily assigned to 0 1 2 ($2_1 3_2$).

Reutt *et al.*⁵¹ also containing more extensive vibrational progressions arising from the \tilde{A}^2A_1 and \tilde{B}^2B_2 states (see, e.g., Refs. 52 and 53 for other photoelectron studies). The \tilde{A}^2A_1 state is, however, known to exhibit the Renner-Teller effect and the \tilde{A}^2A_1 and \tilde{B}^2B_2 states couple strongly with each other through vibronic interactions and are beyond the applicability of our methods. The short vibrational progression of the \tilde{X}^2B_1 band is characteristic of the removal of an electron from the outermost, nonbonding orbital ($2p$ of oxygen) and is expected to be well described by our methods.

The peak positions of the \tilde{X}^2B_1 manifold, including overtones and combination tones, predicted by theory systematically improve with increasing level of approximation from harmonic to the VSCF (direct) and to the VCI (direct) (see Table I). The mean absolute deviation between theory and experiment^{51,54,55} is as large as 321 cm^{-1} in the harmonic approximation, which is greatly reduced to 83 cm^{-1} when VSCF (direct) is used and to mere 21 cm^{-1} at the VCI (direct) level. Our assignments are in agreement with Reutt *et al.*⁵¹ and also with the previous multireference configuration interaction studies by Reuter *et al.*,⁵⁶ Weis *et al.*,⁵⁷ and

Brommer *et al.*⁵⁸ with the exception of the contribution of the 3_2 state to the 6280 cm^{-1} peak (*vide post*). The CCSD(T) method with the cc-pVTZ basis set followed by the VCI (direct) also reproduces accurately the experimental equilibrium geometries^{54,59} and fundamental (anharmonic) frequencies^{54,55,60} for both H_2O and H_2O^+ (Table II).

The predicted FC intensity profiles of the vibrational manifold also approach the experimental spectrum as the theoretical level is raised. The relative intensities of the first two major peaks at 1407 and 3205 cm^{-1} (0.17 and 0.40 eV), assignable to 2_1 (scissors) and 1_1 (symmetric stretch) and both transforming as A_1 , are well reproduced by theory even in the harmonic approximation. However, the small feature at 2775 cm^{-1} (0.34 eV) in between these two peaks, which originates from 2_2 , is completely missing in the harmonic approximation. The VSCF (direct) method corrects this shortcoming, but not with quantitative accuracy ($I_{\text{VSCF}}=0.002$ versus $I_{\text{experiment}}=0.010$). Only at the VCI (direct) level quantitative agreement between theory ($I_{\text{VCI}}=0.011$) and experiment is obtained. According to the VCI (direct), the vibrational wave function of this 2_2 state is expanded as

TABLE II. Equilibrium geometries (bond lengths in \AA and bond angles in degrees) and anharmonic fundamental frequencies (in cm^{-1}) of H_2O (\tilde{X}^1A_1) and H_2O^+ (\tilde{X}^2B_1).

Molecule	Method	r_{OH}	a_{HOH}	ν_1 (A_1)	ν_2 (A_1)	ν_3 (B_2)
H_2O	VCI (direct)/CCSD(T)/cc-pVTZ	0.958	103.6	3670	1608	3751
	Experiment	0.958 ^a	104.5 ^a	3652 ^b	1595 ^b	3756 ^b
H_2O^+	VCI (direct)/CCSD(T)/cc-pVTZ	1.000	108.9	3230	1407	3264
	Experiment	1.001 ^c	108.9 ^c	3213.00 ^c	1408.42 ^d	3253.03 ^c

^aReference 59.

^bReference 60.

^cReference 54.

^dReference 55.

$$\Psi_{2_2}^{\text{VCI}} = 0.96\Psi_{2_2}^{\text{HO}} - 0.18\Psi_{2_3}^{\text{HO}} + 0.13\Psi_{1_1}^{\text{HO}} + 0.09\Psi_{2_1}^{\text{HO}} + \dots, \quad (10)$$

revealing the intensity borrowing by the 2_2 peak primarily from the 1_1 and 2_1 peaks through anharmonic couplings, which are neglected in the harmonic approximation and are not fully accounted for even by the VSCF.

The intensity order of the two peaks at 4593 (1_12_1) and 6280 cm^{-1} (1_2) (which are the two most intense peaks at 0.57 and 0.78 eV in the enlarged part of the spectrum) is predicted incorrectly by the harmonic approximation. The inclusion of the anharmonicity at the VSCF (direct) or VCI (direct) level rectifies this shortcoming, predicting $I_{\text{VSCF}} = 0.021$ (1_12_1) and 0.027 (1_2) in comparison to $I_{\text{experiment}} = 0.016$ (1_12_1) and 0.023 (1_2). It is noteworthy that the first overtone of antisymmetric stretch (3_2), occurring in the proximity of 1_2 and transforming as $B_2 \otimes B_2 = A_1$, contributes appreciably to the intensity of the predicted peak at about 6500 cm^{-1} ($I_{\text{VCI}} = 0.007$). According to the VCI, the wave function of the 3_2 state is written as

$$\Psi_{3_2}^{\text{VCI}} = 0.74\Psi_{3_2}^{\text{HO}} - 0.47\Psi_{1_2}^{\text{HO}} + \dots \quad (11)$$

Hence these two peaks share intensities to a great extent, and together they effectively act as one asymmetric peak. Indeed, the VCI (direct) calculation assigns the peak at 6280 cm^{-1} (0.78 eV) to a compound state of 1_2 and 3_2 having a relative intensity of $0.017 + 0.007 = 0.024$ (the experimental value is 0.023). We therefore suggest that the existence of the 3_2 state might contribute to the apparently more pronounced asymmetry of the observed peak shape (0.78 eV) than the others. However, it should be remembered that the unresolved rotational fine structures are the primary cause of the asymmetry, and the relative positions of these two states may not be calculated to a high enough accuracy to reproduce a peak shape.

Three weak features observed at 4085, 5936, and 7639 cm^{-1} (0.51, 0.74, and 0.95 eV) are also reasonably accurately reproduced by the VCI (direct). The first two are assigned to 2_3 and 1_12_2 in agreement with Reutt *et al.*⁵¹ However, it is found that the peak at 7639 cm^{-1} is more appropriately characterized as 2_13_2 rather than 1_22_1 suggested previously. In general, as the energies of vibrational levels increase, such a simple characterization based on harmonic oscillator normal modes gradually loses its meaning and merit.

Comments on the performance of the QFF approximation are in order. The mean absolute deviations between the VSCF (QFF) and experiment and between the VCI (QFF) and experiment are 81 and 65 cm^{-1} , respectively. They are compared with the corresponding values (83 and 21 cm^{-1}) of the direct method. Hence, the errors inherent to the QFF approximation are masked by those of the VSCF ansatz for the low-lying vibrations of H_2O^+ . When the VCI is used, however, the QFF approximation seems to obstruct the VCI's performance more noticeably. Note, however, that the total number of single-point CCSD(T) executions needed is less than 50 in the QFF approximation as compared to over 700 in the direct method.

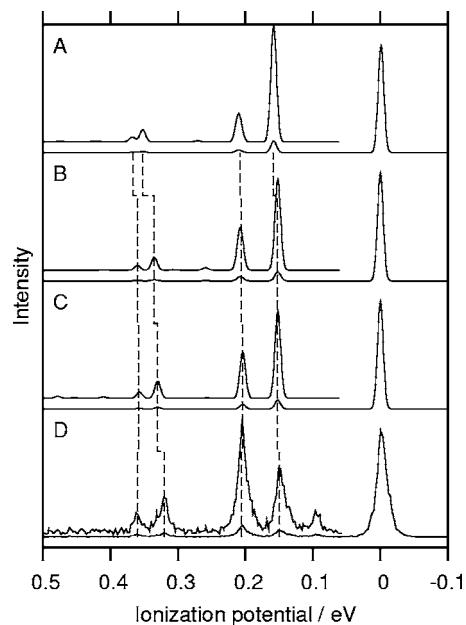


FIG. 2. Vibrational progression of the \tilde{X}^2B_2 photoelectron band of H_2CO (zero of energy is taken as the 0-0 transition position). Calculations based on (A) the harmonic approximation, (B) VSCF (2MR direct) wave functions, and (C) VCI (2MR direct) wave functions are shown in comparison to (D) experiment (Ref. 62). The insert has been multiplied by 10. Each of the theoretical photoelectron peaks has been convoluted with a Gaussian function of FWHM of 0.01 eV.

Table I also compares the two ways of computing FC integrals based on the VCI (direct) wave functions (see Sec. III C). The slight differences in peak positions (in the order of a few reciprocal centimeters) are caused by the use of the harmonic oscillator normal mode basis functions of H_2O to expand H_2O^+ anharmonic wave function in scheme B. Good agreement in the FC integrals between these two schemes mutually validates both. The greater difference is observed in the FC integrals ($I = 0.017$ versus 0.022) and also in the frequency (6333 versus 6342 cm^{-1}) for the 1_2 state, for which the result from scheme A should be trusted.

B. \tilde{X}^2B_2 state of H_2CO^+

The high-resolution photoelectron spectra of H_2CO (and D_2CO) were reported by Niu *et al.* (the bottom panel of Fig. 2),^{61,62} which revealed fine structures that had previously been undetected in the spectra of Baker *et al.*⁶³ In the lowest-lying band system (corresponding to the \tilde{X}^2B_2 state of the cation), five major peaks (excluding the 0-0 transition) are clearly visible. From the low-energy side, they are assigned to the vibrational structures due to $6_1(B_2)$, $3_1(A_1)$, $2_1(A_1)$, $1_1(A_1)$, and $2_13_1(A_1)$, respectively (Table III), according to our calculations (the top three panels of Fig. 2). Our results for the second through fifth peaks support the assignments suggested by Niu *et al.*,⁶² which are, in turn, based on the theoretical work by Domcke and Cederbaum.⁶⁴ Takeshita,⁶⁵ on the basis of his calculations, proposed alternative assignments of the fourth and fifth peaks to $2_13_1(A_1)$ and $2_2(A_1)$, respectively. Our theoretical calculations dismiss Takeshita's assignments in favor of Niu *et al.*

TABLE III. Relative positions (ν in cm^{-1}), relative intensities (I), and assignment of vibrational progression of the \tilde{X}^2B_2 photoelectron band of H_2CO obtained from the CCSD(T)/cc-pVTZ method.

Assignment ^a	Harmonic		VSCF (3MR QFF) ^b		VSCF (2MR direct) ^b		VCI (3MR QFF) ^b		VCI (2MR direct) ^b		VCI (2MR direct) ^c		Expt. ^d	
	ν	I	ν	I	ν	I	ν	I	ν	I	ν	I	ν	I
0 0 0 0 (0_0)	0	1.000	0	1.000	0	1.000	0	1.000	0	1.000	0	1.000	0	1.00
0 0 0 1 (6_1)	853	0.000	847	0.000	839	0.000	823	0.000	833	0.000	763	0.000	764	0.02
0 0 1 0 (3_1)	1277	0.108	1234	0.081	1234	0.084	1214	0.068	1229	0.081	1239	0.084	1204	0.06
0 0 0 2 (6_2) ^e	1707	0.020	1706	0.022	1689	0.023	1621	0.050	1646	0.043	1564	0.042	1501	0.00
0 1 0 0 (2_1) ^e	1678	0.009	1664	0.019	1666	0.020	1680	0.001	1689	0.000	1664	0.026	1656	0.11
0 0 2 0 (3_2)	2554	0.000	2462	0.001	2462	0.001	2416	0.001	2451	0.000	2472	0.000	2396	0.00
1 0 0 0 (1_1)	2841	0.012	2690	0.012	2702	0.012	2653	0.016	2664	0.016	2638	0.017	2580	0.04
0 1 1 0 ($2_1, 3_1$)	2955	0.003	2901	0.004	2904	0.004	2887	0.004	2886	0.006	2907	0.006	2900	0.02
0 2 0 0 (2_2)	3355	0.000	3308	0.000	3308	0.000	3279	0.000	3280	0.000	3309	0.001	3274	0.00

^aQuantum numbers of ν_1 (CH symmetric stretch; A_1), ν_2 (CO stretch; A_1), ν_3 (CH_2 scissors; A_1), and ν_6 (CH_2 rock; B_2).

^bScheme A based on the Franck-Condon integrals of harmonic oscillator wave functions (see text).

^cScheme B based on the anharmonic wave functions of H_2CO and H_2CO^+ both expanded by the harmonic oscillator wave functions of H_2CO (see text).

^dReference 62. The intensities have been estimated from Fig. 2 of the same reference.

^eConsiderable mixing of states has been observed and the theoretical assignments of these two states are interchangeable (see text).

Comparing the simulated spectra in three different approximations in Fig. 2, we notice that the peak positions improve considerably from the harmonic approximation to the VSCF (direct) or VCI (direct). The agreement between the calculated and experimental anharmonic frequencies is within 30 cm^{-1} for the $3_1(A_1)$, $2_1(A_1)$, and $2_1, 3_1(A_1)$ (second, third, and fifth) peaks, while the deviation seen in the harmonic approximation can be over 70 cm^{-1} . For the fourth peak, which arises from the symmetric stretch $1_1(A_1)$, the harmonic frequency (2841 cm^{-1}) is excessively overestimated (the experimental value is 2580 cm^{-1}). The VSCF (direct) and VCI (direct) correct the theoretical values in the right direction (2702 and 2664 cm^{-1}), but the results are still too high by as much as over 80 cm^{-1} . Since the calculated frequency of the 1_1 mode of H_2CO^+ changes only slightly (11 cm^{-1}) upon going from VCI (2MR direct) to VCI (3MR QFF), it is unlikely that the truncation of many-mode expansion (the 2MR approximation) is the cause of this discrepancy. Rather, we are inclined to ascribe this to the inability of the electronic structure theory [CCSD(T)/cc-pVTZ] to describe the relevant part of the PEF with sufficient fidelity. There is also an uncharacteristically large difference in the frequency of the ν_5 mode for H_2CO between theory

(2783 cm^{-1}) and experiment (2843 cm^{-1}) at the 2MR level (Table IV). This is known⁴⁴ to be caused by a Fermi resonance with the $3_1, 6_1$ and $2_1, 6_1$ combination tones, which cannot be adequately addressed unless 3MR or higher is used.

Possibly coupled with the errors in peak positions, the intensities of the vibrational structures do not match the experimental spectrum unlike the excellent agreement in H_2O^+ . The $1_1(A_1)$, and $2_1, 3_1(A_1)$ (fourth and fifth) peaks are reasonably well reproduced by theory, but the intensity order of the $3_1(A_1)$ and $2_1(A_1)$ (second and third) peaks is reversed. The VSCF and VCI seem to alter the relative intensities of the two peaks in the right direction, but not to the extent that the correct order is restored. The $3_1(A_1)$ and $2_1(A_1)$ modes correspond to CH_2 scissors and CO stretching motions. Qualitatively, the intensity of a vibrational structure is expected to be greater when the associated vibrational motion is more proportional to the change in equilibrium geometry from the initial to the final state. Table IV compares the CCSD(T) and experimental equilibrium geometries and frequencies^{62,66–70} of H_2CO and H_2CO^+ . Clearly, the theory exaggerates the widening of HCH angle and underestimates the shortening of the CO bond upon ionization, as compared to the experiments. This apparently explains the overestimation of the

TABLE IV. Equilibrium geometries (bond lengths in Å and bond angles in degrees) and anharmonic fundamental frequencies (in cm^{-1}) of H_2CO (\tilde{X}^1A_1) and H_2CO^+ (\tilde{X}^2B_2).

Molecule	Method	$r_{\text{C=O}}$	$r_{\text{C-H}}$	a_{HCH}	$\nu_1 (A_1)$	$\nu_2 (A_1)$	$\nu_3 (A_1)$	$\nu_4 (B_1)$	$\nu_5 (B_2)$	$\nu_6 (B_2)$
H_2CO	VCI (2MR direct)/ CCSD(T)/cc-pVTZ	1.206	1.096	116.3	2791	1758	1514	1172	2783	1254
	Experiment	1.203 ^a	1.101 ^a	116.2 ^a	2782 ^b	1746 ^b	1500 ^b	1167 ^b	2843 ^b	1250 ^b
H_2CO^+	VCI (2MR direct)/ CCSD(T)/cc-pVTZ	1.196	1.107	121.2	2664	1646	1229	1042	2673	833
	Experiment	1.184, ^c -0.021 ^d	1.123, ^c +0.022 ^d	119.3, ^c +2.4 ^d	2580 ^e	1656 ^e	1204, ^e 1153 ^f	919 ^f	2718 ^f	764, ^e 814 ^f

^aReference 67.

^bReference 69.

^cReference 66.

^dGeometry changes upon ionization (Ref. 68).

^eReference 62.

^fReference 70.

$3_1(A_1)$ peak (CH_2 scissors), the underestimation of the $2_1(A_1)$ peak (CO stretch), and the reversal of the intensity order. However, the experimental geometries^{66,68} have been deduced from cruder FC analyses of photoelectron spectra and, therefore, they may not serve as an independent check of the theoretical prediction. In fact, it has proven to be unexpectedly difficult to reproduce the equilibrium geometries of H_2CO^+ with the same accuracy achievable for H_2CO .⁷¹ An accurate experimental determination of the geometrical parameters of H_2CO^+ , independent of photoelectron spectral measurements, is warranted.

The most troubling aspect of the spectrum is the weak feature around 0.1 eV above the 0-0 transition, which we assign to $6_1(B_2)$. Niu *et al.* assigned this to $4_1(B_1)$, an out-of-plane CH_2 wagging mode. On this basis, they raised a possibility that H_2CO^+ in its ground electronic state assumed nonplanar equilibrium geometry. Later, a thorough computational study of geometries and harmonic vibrational frequencies of H_2CO^+ appeared,⁷² in which Bruna *et al.* concluded that the peak in question (764 cm^{-1}) could only correspond to $6_1(B_2)$, an in-plane CH_2 rocking mode ($841\text{--}856\text{ cm}^{-1}$ from their calculations; 833 cm^{-1} from our direct VCI calculation), which was further supported by Liu *et al.*⁷⁰ Our calculations support the assignment and do not find a nonplanar geometry of H_2CO^+ , both in agreement with Bruna *et al.* and Liu *et al.* Therefore, the appearance of this peak in the photoelectron spectra no longer implies nonplanar geometry. However, the transition to the $6_1(B_2)$ state (unlike the even overtones of ν_6 that transform as A_1) is still symmetry forbidden within the Born-Oppenheimer separation and cannot be accounted for by our calculations that give exactly zero FC factor for this transition.

One plausible explanation is that the nonadiabatic coupling between \tilde{X}^2B_2 and \tilde{B}^2A_1 states of H_2CO^+ through the $6_1(B_2)$ mode makes this latter mode weakly vibronically active in its photoelectron spectra. This might be indirectly supported by the electronic absorption spectra of H_2CSi (Ref. 73) and H_2CGe ,⁷⁴ which also exhibit the 6_1 (CH_2 rock) (B_2) vibrational progression due to a vibronic coupling between the ground state and a nearby 1A_1 state. For the vinylidene anion (H_2CC^-), however, Stanton and Gauss⁷⁵ showed that a CCSD(T) calculation with anharmonicity accounted for at the second-order perturbation level could unequivocally establish the assignment of a feature observed at $450\pm 30\text{ cm}^{-1}$ in its photoelectron spectra⁷⁶ to the *first overtone* of CH_2 rocking mode $6_2(A_1)$ (479 cm^{-1} according to theory) of H_2CC . The experimental spectra⁷⁶ did not show evidence of vibronic activity of the 6_1 mode in H_2CC .

The comparison between schemes A and B indicates that, when the agreement in frequencies (energies) is good, the computed FC integrals from the two approaches also agree well with each other and can be trusted. The largest discrepancy has been observed for the fundamentals and overtones of ν_6 . This is caused by the substantial frequency change in ν_6 upon ionization ($1250\text{--}764\text{ cm}^{-1}$), making the harmonic oscillator wave function of H_2CO ν_6 an inadequate basis for expanding the anharmonic wave function of H_2CO^+ ν_6 . The apparent good agreement in the 6_1 and 6_2 state positions between scheme B and experiment is, therefore, for-

titious. Furthermore, the 6_2 and 2_1 states, both transforming as A_1 , exhibit a varied degree of intensity sharing, causing the calculated FC integrals to be sensitively dependent on the relative energies of the two states and hence on various theoretical treatments. From the experimental viewpoint also, the two peaks (at 1501 and 1656 cm^{-1}) overlap and hence it may not be very meaningful to try to pinpoint which peak is assigned to the 6_2 or 2_1 state and how much of the total intensity comes from each state.

V. CONCLUSION

The two proposed methods for *anharmonic* FC integral evaluations require only a set of single-point energies from an electronic structure theory, which they use to generate VSCF and VCI wave functions expanded by normal mode harmonic oscillator basis functions that are unambiguously defined for general polyatomic molecules. They need neither an *ad hoc* coordinate system to represent a PEF in a convenient analytical form nor to be tied to a particular approximation or computer program for electronic structure calculations. Their limitation in their current implementation (not a conceptual one), however, is the lack of small couplings between various degrees of freedom such as nonadiabatic (vibronic) interactions, Renner-Teller and Jahn-Teller effects, and rovibrational coupling.

The two methods differ from each other in whether the vibrational wave functions of initial and final states are expanded by harmonic oscillator bases of the respective states (scheme A) or by a harmonic oscillator or VSCF basis of one state (scheme B). Three competing factors that determine the accuracy of scheme B are the extent of geometry and frequency changes and normal mode rotation between the two states, the fidelity of PEFs in representing the relevant areas of the potential energy surfaces, and the truncation order of VCI. In practice, when the energies of the states computed by the two schemes agree well, the associated FC integrals from scheme B should also be reliable.

The methods have enabled a quantitative interpretation of the \tilde{X}^2B_1 photoelectron system of H_2O , revealing the importance of intensity borrowing and anharmonic mode couplings in explaining some small peaks. The \tilde{X}^2B_2 photoelectron system of H_2CO shows unexpectedly noticeable disagreement between theory and experiment in peak positions and relative intensities, proving to be a rather delicate problem for such a small and basic molecule. It demands a more extensive electronic and vibrational structure theory that possibly needs to account for the nonadiabatic (vibronic) effects.

ACKNOWLEDGMENTS

The authors affiliated with the University of Florida thank the financial support from the U. S. Department of Energy (Grant No. DE-FG02-04ER15621) and from the University of Florida Division of Sponsored Research. The authors are also indebted to Dr. Ajith D. Perera for assistance with the ACES II program and to Dr. Martin Vala and Dr. Jan Szczepanski for an insightful discussion on the spectral band assignments of H_2CO^+ .

- ¹J. Franck, *Trans. Faraday Soc.* **21**, 536 (1925).
- ²E. U. Condon, *Phys. Rev.* **32**, 858 (1928).
- ³J. M. Bowman, *Acc. Chem. Res.* **19**, 202 (1986).
- ⁴M. A. Ratner and R. B. Gerber, *J. Phys. Chem.* **90**, 20 (1986).
- ⁵J. M. Bowman, K. Christoffel, and F. Tobin, *J. Phys. Chem.* **83**, 905 (1979).
- ⁶L. S. Norris, M. A. Ratner, A. E. Roitberg, and R. B. Gerber, *J. Chem. Phys.* **105**, 11261 (1996).
- ⁷O. Christiansen, *J. Chem. Phys.* **120**, 2149 (2004).
- ⁸J. A. Pople, M. Head-Gordon, D. J. Fox, K. Raghavachari, and L. A. Curtiss, *J. Chem. Phys.* **90**, 5622 (1989).
- ⁹S. Carter, S. J. Culik, and J. M. Bowman, *J. Chem. Phys.* **107**, 10458 (1997).
- ¹⁰G. M. Chaban, J. O. Jung, and R. B. Gerber, *J. Chem. Phys.* **111**, 1823 (1999).
- ¹¹K. Yagi, T. Taketsugu, and K. Hirao, *J. Chem. Phys.* **116**, 3963 (2002).
- ¹²T. E. Sharp and H. M. Rosenstock, *J. Chem. Phys.* **41**, 3453 (1964).
- ¹³S. H. Lin, *J. Chem. Phys.* **44**, 3759 (1966).
- ¹⁴J. Katriel, *J. Phys. B* **3**, 1315 (1970).
- ¹⁵L. S. Cederbaum and W. Domcke, *J. Chem. Phys.* **64**, 603 (1976).
- ¹⁶E. V. Doktorov, I. A. Malkin, and V. I. Man'ko, *J. Mol. Spectrosc.* **64**, 302 (1977).
- ¹⁷S. Mukamel, S. Abe, Y. J. Yan, and R. Islampour, *J. Phys. Chem.* **89**, 201 (1985).
- ¹⁸H. Kupka and P. H. Cribb, *J. Chem. Phys.* **85**, 1303 (1986).
- ¹⁹D. Gruner and P. Brumer, *Chem. Phys. Lett.* **138**, 310 (1987).
- ²⁰M. Roche, *Chem. Phys. Lett.* **168**, 556 (1990).
- ²¹P. T. Ruhoff, *Chem. Phys.* **186**, 355 (1994).
- ²²R. Berger, C. Fischer, and M. Klessinger, *J. Phys. Chem. A* **102**, 7157 (1998).
- ²³P. T. Ruhoff and M. A. Ratner, *Int. J. Quantum Chem.* **77**, 383 (2000).
- ²⁴K. M. Ervin, T. M. Ramond, G. E. Davico, R. L. Schwartz, S. M. Casey, and W. C. Lineberger, *J. Phys. Chem. A* **105**, 10822 (2001).
- ²⁵H. Kikuchi, M. Kubo, N. Watanabe, and H. Suzuki, *J. Chem. Phys.* **119**, 729 (2003).
- ²⁶M. Dierksen and S. Grimme, *J. Chem. Phys.* **122**, 244101 (2005).
- ²⁷H. Torii and M. Tasumi, *J. Chem. Phys.* **101**, 4496 (1994).
- ²⁸D. K. W. Mok, E. P. F. Lee, F.-T. Chau, D. C. Wang, and J. M. Dyke, *J. Chem. Phys.* **113**, 5791 (2000).
- ²⁹D. K. W. Mok, E. P. F. Lee, F.-T. Chau, and J. M. Dyke, *J. Chem. Phys.* **120**, 1292 (2004).
- ³⁰F.-T. Chau, D. K. W. Mok, E. P. F. Lee, and J. M. Dyke, *J. Chem. Phys.* **121**, 1810 (2004).
- ³¹E. P. F. Lee, D. K. W. Mok, F.-T. Chau, and J. M. Dyke, *J. Chem. Phys.* **121**, 2962 (2004).
- ³²J. M. Bowman, X. Huang, L. B. Harding, and S. Carter, *Mol. Phys.* **104**, 33 (2006).
- ³³A. Hazra and M. Nooijen, *Int. J. Quantum Chem.* **95**, 643 (2003).
- ³⁴A. Hazra, H. H. Chang, and M. Nooijen, *J. Chem. Phys.* **121**, 2125 (2004).
- ³⁵A. Hazra and M. Nooijen, *J. Chem. Phys.* **122**, 204327 (2005).
- ³⁶A. Hazra and M. Nooijen, *Phys. Chem. Chem. Phys.* **7**, 1759 (2005).
- ³⁷J. M. Luis, D. M. Bishop, and B. Kirtman, *J. Chem. Phys.* **120**, 813 (2004).
- ³⁸J. M. Luis, M. Torrent-Sucarrat, M. Solà, D. M. Bishop, and B. Kirtman, *J. Chem. Phys.* **122**, 184104 (2005).
- ³⁹K. Raghavachari, G. W. Trucks, J. A. Pople, and M. Head-Gordon, *Chem. Phys. Lett.* **157**, 479 (1989).
- ⁴⁰J. D. Watts, J. Gauss, and R. J. Bartlett, *J. Chem. Phys.* **98**, 8718 (1993).
- ⁴¹T. H. Dunning, Jr., *J. Chem. Phys.* **90**, 1007 (1989).
- ⁴²J. F. Stanton, J. Gauss, J. D. Watts *et al.*, ACES II, Quantum Theory Project, University of Florida; J. Almlöf and P. R. Taylor, VMOL; P. Taylor, VPROPS; T. Helgaker, H. J. Aa. Jensen, P. Jørgensen, J. Olsen, and P. R. Taylor, ABACUS.
- ⁴³K. Yagi, SINDO, University of Tokyo, Tokyo, Japan, 2006.
- ⁴⁴K. Yagi, T. Taketsugu, K. Hirao, and M. S. Gordon, *J. Chem. Phys.* **113**, 1005 (2000).
- ⁴⁵J. C. Light and T. Carrington, *Adv. Chem. Phys.* **114**, 263 (2000).
- ⁴⁶K. Yagi, K. Hirao, T. Taketsugu, M. W. Schmidt, and M. S. Gordon, *J. Chem. Phys.* **121**, 1383 (2004).
- ⁴⁷T. A. Ruden, P. R. Taylor, and T. Helgaker, *J. Chem. Phys.* **119**, 1951 (2003).
- ⁴⁸M. Yamaguchi, T. Momose, and T. Shida, *J. Chem. Phys.* **93**, 4211 (1990).
- ⁴⁹S. Iwata (private communication).
- ⁵⁰F. Duschinsky, *Acta Physicochim. URSS* **7**, 551 (1937).
- ⁵¹J. E. Reutt, L. S. Wang, Y. T. Lee, and D. A. Shirley, *J. Chem. Phys.* **85**, 6928 (1986).
- ⁵²L. Karlsson, L. Mattsson, R. Jadrny, R. G. Albridge, S. Pinchas, T. Bergmark, and K. Siegbahn, *J. Chem. Phys.* **62**, 4745 (1975).
- ⁵³R. N. Dixon, G. Duxbury, J. W. Rabalais, and L. Åsbrink, *Mol. Phys.* **31**, 423 (1976).
- ⁵⁴B. M. Dinelli, M. W. Crofton, and T. Oka, *J. Mol. Spectrosc.* **127**, 1 (1988).
- ⁵⁵P. R. Brown, P. B. Davies, and R. J. Stickland, *J. Chem. Phys.* **91**, 3384 (1989).
- ⁵⁶W. Reuter, M. Perić, and S. D. Peyerimhoff, *Mol. Phys.* **74**, 569 (1991).
- ⁵⁷B. Weis, S. Carter, P. Rosmus, H.-J. Werner, and P. J. Knowles, *J. Chem. Phys.* **91**, 2818 (1989).
- ⁵⁸M. Brommer, B. Weis, B. Follmeg, P. Rosmus, S. Carter, N. C. Handy, H.-J. Werner, and P. J. Knowles, *J. Chem. Phys.* **98**, 5222 (1993).
- ⁵⁹A. R. Hoy and P. R. Bunker, *J. Mol. Spectrosc.* **74**, 1 (1979).
- ⁶⁰G. Herzberg, *Electronic Spectra and Electronic Structure of Polyatomic Molecules*. (Van Nostrand, New York, 1966).
- ⁶¹B. Niu, D. A. Shirley, Y. Bai, and E. Daymo, *Chem. Phys. Lett.* **201**, 212 (1993).
- ⁶²B. Niu, D. A. Shirley, and Y. Bai, *J. Chem. Phys.* **98**, 4377 (1993).
- ⁶³A. D. Baker, C. Baker, C. R. Brundle, and D. W. Turner, *Int. J. Mass Spectrom. Ion Phys.* **1**, 285 (1968).
- ⁶⁴W. Domcke and L. S. Cederbaum, *J. Chem. Phys.* **64**, 612 (1976).
- ⁶⁵K. Takeshita, *J. Chem. Phys.* **94**, 7259 (1991).
- ⁶⁶G. L. Goodman and J. Berkowitz, in *Molecular Ions: Geometric and Electronic Structures*, edited by J. Berkowitz and K.-O. Groeneveld (Plenum, New York, 1983), p. 69.
- ⁶⁷D. J. Clouthier and D. A. Ramsay, *Annu. Rev. Phys. Chem.* **34**, 31 (1983).
- ⁶⁸F. T. Chau and C. A. McDowell, *Spectrochim. Acta, Part A* **46**, 723 (1990).
- ⁶⁹R. J. Bouwens, J. A. Hammerschmidt, M. M. Grzeskowiak, T. A. Stegink, P. M. Yorba, and W. F. Polik, *J. Chem. Phys.* **104**, 460 (1996).
- ⁷⁰J. Liu, H.-T. Kim, and S. L. Anderson, *J. Chem. Phys.* **114**, 9797 (2001).
- ⁷¹The calculated CO and CH bond lengths and HCH bond angle are 1.197 Å, 1.107 Å, and 121.1° at the coupled-cluster with singles, doubles, and triples (CCSDT) level with the cc-pVTZ basis set; 1.192 Å, 1.103 Å, and 121.4° at the ionization-potential equation-of-motion CCSD (IP-EOM-CCSD) method with the cc-pVTZ basis set; and 1.200 Å, 1.114 Å, and 121.2° at the CCSD(T) (frozen core) level with the aug-cc-pVTZ basis set. None of these results seems to be an essential improvement over the CCSD(T)/cc-pVTZ result in comparison with the experimental data in Table IV.
- ⁷²P. J. Bruna, M. R. J. Hachey, and F. Grein, *Mol. Phys.* **94**, 917 (1998).
- ⁷³W. W. Harper, K. W. Waddell, and D. J. Clouthier, *J. Chem. Phys.* **107**, 8829 (1997).
- ⁷⁴D. A. Hostutler, T. C. Smith, H. Li, and D. J. Clouthier, *J. Chem. Phys.* **111**, 950 (1999).
- ⁷⁵J. F. Stanton and J. Gauss, *J. Chem. Phys.* **110**, 6079 (1999).
- ⁷⁶K. M. Ervin, J. Ho, and W. C. Lineberger, *J. Chem. Phys.* **91**, 5974 (1989).